Docking-Based Development of Purine-like Inhibitors of Cyclin-Dependent Kinase-2

Michal Otyepka,[†] Vladimír Kryštof,[‡] Libor Havlíček,[§] Věra Siglerová,[‖] Miroslav Strnad,[‡] and Jaroslav Koča[*,⊥]

Department of Inorganic and Physical Chemistry, Faculty of Science, Palacký University, tř. Svobody 8, 771 46 Olomouc, Czech Republic; Laboratory of Growth Regulators, Faculty of Science, Palacký University & Institute of Experimental Botany, Šlechtitelů 11, 783 71 Olomouc, Czech Republic; Central Radioisotope Laboratory, Medical Faculty 1, Charles University, Na bojišti 3, 121 08 Praha 2, Czech Republic; Isotope Laboratory, Institute of Experimental Botany, Videňská 1083, 14220 Praha 4, Czech Republic; and Laboratory of Biomolecular Structure and Dynamics, Faculty of Science, Masaryk University, Kotlářská 2, 611 37 Brno, Czech Republic

The cell division cycle is controlled by cyclin-dependent kinases (cdk), which consist of a catalytic subunit (cdk1-cdk8) and a regulatory subunit (cyclin A−H). Purine-like inhibitors of cyclin-dependent kinases have recently been found to be of potential use as anticancer drugs. Rigid and flexible docking techniques were used for analysis of binding mode and design of new inhibitors. X-ray structures of three (ATP, olomoucine, roscovitine) cdk2 complexes were available at the beginning of the study and were used to optimize the docking parameters. The new potential inhibitors were then docked into the cdk2 enzyme, and the enzyme/inhibitor interaction energies were calculated and tested against the assayed activities of cdk1 (37 compounds) and cdk2 (9 compounds). A significant rank correlation between the activity and the rigid docking interaction energy has been found. This implies that (i) the rigid docking can be used as a tool for qualitative prediction of activity and (ii) values obtained by the rigid docking technique into the cdk2 active site can also be used for the prediction of cdk1 activity. While the resulting geometries obtained by the rigid docking are in good agreement with the X-ray data, the flexible docking did not always produce the same inhibitor conformation as that found in the crystal.

Introduction

The cell division cycle is controlled by cyclin-dependent kinases (cdk), which consist of a catalytic subunit (cdk1−cdk8) and a regulatory subunit (cyclin A−cyclin H). These proteins are regulated in several ways: subunit production, complex formation, (de)phosphorylation, cellular localization, and interaction with various natural protein inhibitors. Recently, a deregulation of cdks has been proved in human primary tumors and in tumor cell lines.[1] The discovery evoked a strong interest in inhibitors of cdk that could play a role in the therapy of cancers. Several types of cdk inhibitors have so far been described: staurosporine,[2] flavopiridole (L86−8275),[3] butyrolactone-1,[4] purine derivatives,[5] indirubin,[6] paullones,[7] and others.[8,9]

Molecular modeling techniques that can help us to predict the leading compound are more and more frequently used in the development of medicinal drugs. Many drugs produce their effect by interacting with a biological target such as active sites of enzymes or DNA, and the interaction is in many cases caused by nonbond forces. Therefore, molecular docking techniques based on a nonbond force field can be used to predict orientation and complementarity of the ligand to its target.[10]

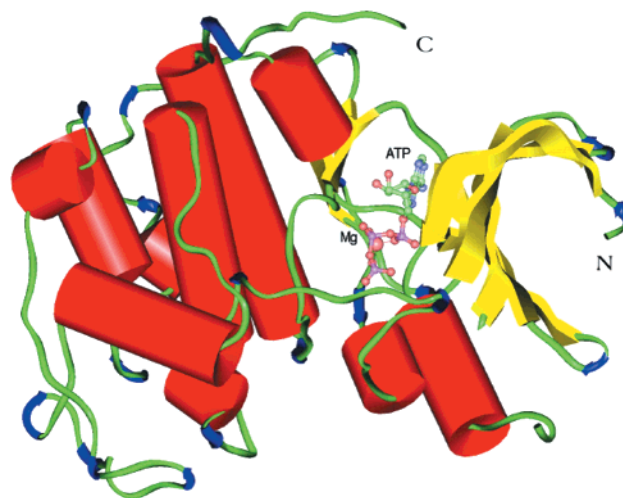Molecular docking starts with the knowledge of the

Figure 1. A Kabsch−Sander model of the structure of ATP-cdk2 complex. N and C termini of the protein are denoted by N and C, respectively; ATP molecule is shown with coordinated Mg^{2+} ion. The C-terminal domain consists primarily of α-helices (cylinders) and N-terminal domain consists predominantly of β-sheets (ribbons).

active site or even with information about the structure of the ligand−receptor complex. In the past few years, the structures of some cdk2 complexes have been published.[11,12] The cdk2 that regulates the G1/S cell cycle phase transition and DNA replication consists of two lobes, a smaller N-terminal domain and a larger C-terminal domain, and ATP and all inhibitors bind in the deep cleft between the lobes (Figures 1 and 2).

* Corresponding author. Tel: 420 5 41129310. Fax: 420 5 41211214. E-mail: jkoca@chemi.muni.cz.
† Palacký University.
‡ Palacký University & Institute of Experimental Botany.
§ Charles University.
‖ Institute of Experimental Botany.
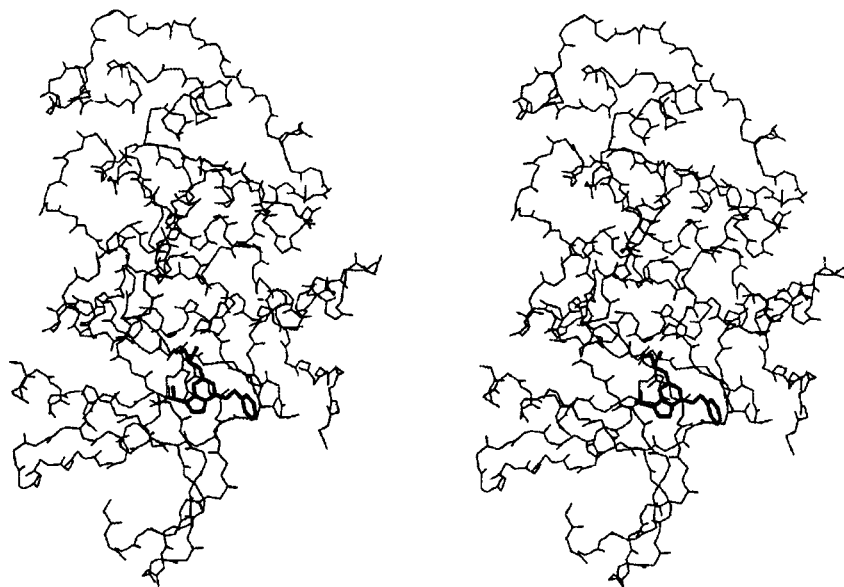⊥ Masaryk University.

Figure 2. A stereoview of cdk2 (backbone) complexed with roscovitine (represented by thick line).
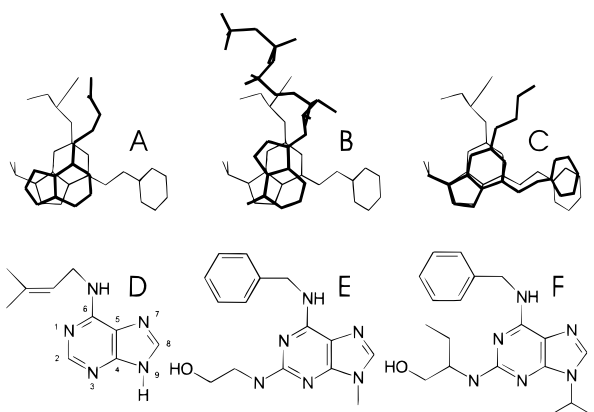

Figure 3. Comparison of (A) 6-(3,3-dimethylallylamino)purine (IPA), (B) ATP, and (C) olomoucine orientation (thick lines) with roscovitine (thin lines) orientation in the active site. Structures of (D) 6-(3,3-dimethylallylamino)purine, (E) olomoucine, and (F) roscovitine.

There are no significant differences in domain orientations between the ligand−enzyme complexes and the apoenzyme, but there are considerable differences in the orientation of different types of ligand.[13] The differences in the binding of ATP and adenine-based inhibitors are shown in Figure 3. The molecules of 2,6,9-substituted purines, 6-[(3-chloro)anilino]-2-(*R*)-[[1-(hydroxymethyl)-2-(methyl)propyl]amino]-9-isopropylpurine (purvalanol B), 6-(benzylamino)-2-[(hydroxyethyl)amino]-9-methylpurine (olomoucine, Figure 3E), and 6-(benzylamino)-2-(*R*)-[[1-(hydroxymethyl)propyl]amino]-9-isopropylpurine (roscovitine, Figure 3F) are very similarly positioned in the active site. On the other hand, the positions of mono- (isopentenyladenine (IPA), Figure 3D) and di- (ATP) substituted purines in the cavity are very different from each other. This supports the conclusion that a similar substitution of 2,6,9-substituted purines should lead to a similar positioning in the active site, and, consequently, to the same binding mode. Each binding mode of purine derivatives is characterized by several H-bonds to the backbone of the kinase active site. The ATP binding mode (Figure 3B) is characterized by two H-bonds, (ATP)N[6]H...OC(Glu81) and (ATP)-

N1...HN(Leu83). The roscovitine binding mode (Figure 3C) is characterized also by two H-bonds, (roscovitine)-N7...HN(Leu83) and (roscovitine)N[6]H...OC(Leu83). Purvalanol B, an efficient inhibitor, employs the roscovitine binding mode and, moreover, it creates another H-bond between the acidic C8 carbon and kinase backbone, (purvalanol B)C8H...OC(Glu81). Finally, the IPA binding mode (Figure 3A) is defined by three H-bonds, (IPA)N3...HN(Leu83), (IPA)N9H...OC(Glu81), and (IPA)N7...HN(terminal group of Lys33). Recently, an X-ray paper dealing with the determinants of the binding modes has been published.[14]

Here we report on the testing of molecular docking techniques on cdk2. Using rigid docking, we predict activities and ways to enhance them for the set of new inhibitors based on 2,6,9-purine derivatives.

Molecular Modeling Methods

Receptor Preparation. X-ray structures of the apo-cdk2 (Brookhaven Protein Data Bank access code 1hcl), the ATP−cdk2 complex (1hck), the ATP-activated cdk2/cyklinA (1jst), and the purvalanol B−cdk2 (1ckp) complex were obtained from the Protein Data Bank. X-ray structures of the cdk2−roscovitine (complex **I**), −olomoucine (**II**), and −6-(3,3-dimethylallylamino)-purine (IPA) (**III**) complexes were kindly provided by Prof. S.-H. Kim. Receptors were prepared for docking in such a way that all heteroatoms (i.e., nonreceptor atoms such as water, ions, etc.) were removed. This was done with one exception, complex **I**, where the 534th water molecule was kept because it creates a strong hydrogen bond with the enzyme and is positioned deep in the cleft. Insight II software (MSI)[15] was used to add hydrogen atoms and to generate Sybyl (Tripos) mol2 files. The receptor active site for DOCK[16] was represented by spheres that were constructed on the Connolly surface of the receptor with 1 Å probe size. The spheres positioned outside the active site were deleted manually. Table 1 shows the most important rigid docking parameters. A typical rigid docking experiment consumed about 400 s of computer time (SGI Indigo[2] Extreme, R4400).

Table 1. Parameters for Rigid Docking (DOCK 4.0)

parameter	value	parameter	value	parameter	value
bump_maximum	4	attractive_exponent	6	total_orientations	5000
energy_cutoff_distance	15	repulsive_exponent	12	nodes_minimum	4
dielectric_factor	4	energy_minimize	yes	nodes_maximum	10
distance_dependent	yes	maximum_cycles	10	distance_tolerance	0.25
random_search	yes	energy_convergence	0.1	distance_minimum	2
uniform_sampling	yes	maximum_iterations	100	grid_points	10^6

Table 2. Parameters for Rigid and Flexible Docking (AutoDock 2.4)

parameter	value	parameter	value
initial RT	616	cycles	55
RT reduction factor	0.95	steps accepted	35000
number of runs	15	steps rejected	35000

Ligand Preparation. The ligands were minimized by the semiempirical PM3 method (HyperChem[17]). The crystal structure conformations of roscovitine, olomoucine, and purvalanol B were used as initial geometries for the optimization. A 0.05 kcal/molÅ gradient was used as the terminating condition; there were no significant differences in interaction energies on using a lower gradient. Empirical partial atomic charges were taken from the CVFF force field with the assistance of Insight II software. The docking experiments, where the set of Mulliken partial atomic charges calculated for the PM3 optimized structure gave results with less negative binding energy in comparison with the docking experiments where empirical partial charges, were employed.

Binding Mode Analysis. The flexible docking technique was used for the binding mode analysis. As flexible docking implemented in DOCK consumed considerable computer resources, we have used the flexible docking based on Monte Carlo simulated annealing as implemented in AutoDock.[18] The flexible docking experiment with 12 active torsions (roscovitine) consumed about 25 h (SGI Indigo^2 Extreme, R4000) of computer time. Table 2 shows the parameters used for docking.

Results and Discussion

Receptor Hunting and Parameter Optimization. First of all, a search for the best receptor structure for molecular docking was performed. The structures of apo-cdk2, ATP−cdk2, the phosphorylated complex of ATP−cdk2/cyclin A, and roscovitine−cdk2 complexes were used as possible candidates. They were tested by a rigid docking of the ligand into the receptor. The key criterion describing the quality of the dock was the convergence in graphs in which the interaction energy is plotted against rmsd (root-mean-square deviation). An example of such a graph is shown in Figure 4. The best results for olomoucine and roscovitine were obtained using the receptor from the complex **I**. The results for 6-(3,3-dimethylallylamino)purine were also acceptable. The parameters for docking, especially dielectric properties and Lennard-Jones potential, were optimized by running several docks on the best receptor structure. The following parameters and their combinations were varied: Lennard-Jones potential 10−12, 6−12; dielectric constant scale factor D (1, 2, 3, 4, 6); and distance-dependent dielectric scale factor D (1, 2, 3, 4, 6). It was found out that the 6−12 Lennard-Jones potential and the distance-dependent dielectric constant with the dielectric factor of 4 are the best parameters
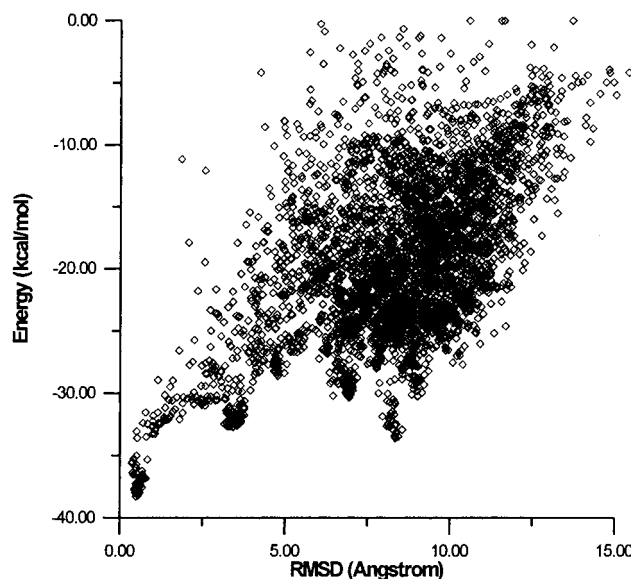

Figure 4. Interaction energies (kcal mol^{-1}), as calculated for the 5000 docked roscovitine-cdk2 complexes using DOCK, are plotted against the rmsd (Å), from the roscovitine orientation in the crystal complex. The docking experiments converge to four binding modes (with the rmsd of 0.41, 3.5, 6.5, and 8 respectively), the best one being identical with the X-ray structure.

for the docking of 2,6,9-purine derivatives into the cdk2 active site. The optimized parameters for the docking are collected in Table 1.

Relationships between the cdk2 Activity and the Interaction Energy. Several compounds with various 2,6,9-substituents were tested for their inhibition activity. Interaction energies for these compounds were taken from the rigid docking, and the relationship between the interaction energy (E) and activity (IC$_{50}$) (Table 3) was analyzed. Since there is no direct significant relationship between the two variables, we have calculated Spearman's rank order correlation coefficient ρ using eq 1.

$$\rho = 1 - \frac{6 \sum_{i}^{n} [r(x_i) - r(y_i)]^2}{n^3 - n} \tag{1}$$

where n is the number of pairs ($n = 8$ in our case), $r(x_i)$ and $r(y_i)$ are the rank of the activity and the interaction energy of the ith sample in the testing set.

The value obtained ($\rho = 0.643$) is the same as the critical value at the 0.05 level of significance.[19] It implies that the rigid docking experiments can be used for qualitative activity prediction. However, a larger set of samples will be necessary to prove this statement.

Relationships between the cdk1 Activity and the Interaction Energy. The structure of cdk1 has not

Table 3. Comparison of IC$_{50}$ Values for Various Purine Derivatives Tested on cdk2 and cdk1 with Interaction Energies from the Docking Experiment

	compound	IC$_{50}$, μM		E^a
		cdk1	cdk2	
1	6-(benzylamino)-2-[(3-hydroxypropyl)amino]-9-isopropylpurine	2.5	0.8	−39.9
2	6-(benzylamino)-2(*R*)-[(2-hydroxypropyl)amino]-9-isopropylpurine	1.1	0.2	−34.0
3	6-(3-hydroxybenzylamino)-2-[[(1-hydroxymethyl)-2-(methyl)propyl]amino]-9-isopropylpurine	0.1	0.03	−38.5
4	6-(benzylamino)-2-[(2-hydroxyethyl)amino]-9-isopropylpurine	9.4	8.0	−32.5
5	6-(benzylamino)-2-[(2-hydroxyethyl)amino]-9-methylpurine	4.6	1.2	−30.8
6	6-(cyclopentylamino)-2-[(3-hydroxypropyl)amino]-9-isopropylpurine	2.4	0.9	−30.3
7	6-amino-2-[(3-hydroxypropyl)amino]-9-isopropylpurine	10	2.4	−27.7
8	6-(adamantylamino)-2-[(3-hydroxypropyl)amino]-9-isopropylpurine^b	>100	>100	−32.7
9	6-(benzylamino)-9-isopropylpurine	3.5	4.5	−28.1
10	6-(2-hydroxybenzylamino)-2-[[1-(hydroxymethyl)-2-(methyl)propyl]amino]-9-ispropylpurine^b	0.01	−	−34.0

^{a} *E* denotes the interaction energy of compound's complex with cdk2 (in kcal/mol). ^{b} Not used for cdk2 energy rank order correlation.
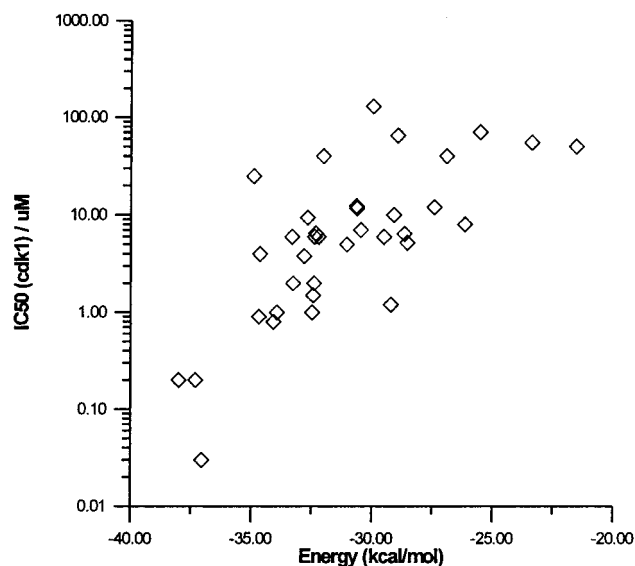
Figure 5. A plot of the inhibitory activity IC$_{50}$ for cdk1 (μM) vs the interaction energy computed for the active site of cdk2 (kcal mol^{-1}).

yet been resolved. The high degree of primary sequence homology between cdk2 and cdk1 (65.5%) suggests that the active sites of these enzymes could be very similar. Therefore, the relationship between the inhibitor/cdk2 interaction energy and the cdk1 assayed activity was tested. Thirty-seven 2,6,9-derivatives of purine were docked into the cdk2 active site, and the interaction energies were computed and compared with activities using Spearman rank correlation. The calculated value $\rho = 0.685$ again implies that the rank of the activities is closely bound to the rank of interaction energies (the critical value for the 0.01 level of probability is <0.4). Figure 5 shows the plot of measured activities (IC$_{50}$) vs calculated interaction energies. However, we did not find any other simple direct relationship between the activity and the interaction energy.

Searching for New Inhibitors. We have analyzed the influence of purine ring substitution in positions 1, 2, 3, 8, and 9 on the inhibitor activity; the results for 2, 8, and 9 positions are collected in Tables 4−6. The docking experiments show that the C8 substituent must be small, because a bulky substituent causes a considerable difference of the ligand orientation in the cavity. For example, methyl and chloro derivatives were positioned quite differently from roscovitine. All the small substituents tested exhibited more negative interaction

Table 4. Influence of the C2 Substituent on the Interaction Energy of 6-(Benzylamino)-9-isopropylpurine

C2 substituent	E	ΔE^a
Cl	−28.8	−7.6
HS	−30.1	−6.3
H$_3$CS	−30.6	−5.8
H$_2$NNH	−30.9	−5.5
HOCH$_2$(Ph)CHNH	−31.4	−5.0
HOCH$_2$[*S*](OH)CHNH	−32.5	−3.9
HO(CH$_2$)$_2$NH	−32.5	−3.9
HO(CH$_2$)$_2$S	−32.6	−3.8
H$_2$N(CH$_2$)$_2$NH	−32.7	−3.7
(CH$_3$)$_2$N	−33.0	−3.4
HO(CH$_2$)$_3$N(CH$_3$)	−33.1	−3.3
H$_2$N(CH$_2$)$_3$NH	−33.5	−2.9
[*S*]HO(CH$_3$)CHCH$_2$NH	−34.0	−2.4
PhCH$_2$NH	−34.4	−2.0
HOCH$_2$[*R*](OH)CHNH	−35.3	−1.1

^{a} ΔE = interaction energy of roscovitine (-36.4 kcal mol^{-1}) − interaction energy of the derivative.

Table 5. Influence of the C8 Substituent on the Interaction Energy (*E*/kcal mol^{-1}) of 6-(Benzylamino)-2-(*R*)-[[1-(hydroxymethyl)propyl]amino]-9-isopropylpurine (roscovitine)

C8 substituent	E	ΔE^a
NH$_2$	−33.7	−2.7
OH	−34.2	−2.2
CN	−34.4	−2.0

^{a} ΔE = interaction energy of roscovitine (-36.4 kcal mol^{-1}) − interaction energy of the derivative.

Table 6. Influence of the N9 Substituent on the Interaction Energy of 6-(Benzylamino)-2-(*R*)-[[1-(hydroxymethyl)propyl]aminopurine^a

N9 substituent	E	ΔE^a
F$_3$C	−30.1	−6.3
H$_3$C	−32.7	−3.7
H$_5$C$_2$	−33.9	−2.5
Cl$_3$C	−36.3	−0.1
(NH$_2$)$_2$CH	−39.3	2.9
Cl$_2$CH	−39.5	3.1
−OOC	−40.7	4.3

^{a} ΔE = interaction energy of roscovitine (-36.4 kcal mol^{-1}) − interaction energy of the derivative.

energies than the roscovitine (Table 5). This should imply a lower activity, although the active site flexibility could also influence the binding of compounds substituted by bulky groups.

The docking and experimental data show that the N9-substitution is important for the positive binding, and isopropyl appears to have an appropriate shape (cf. ref 20). The interaction energies of methyl, ethyl, etc.
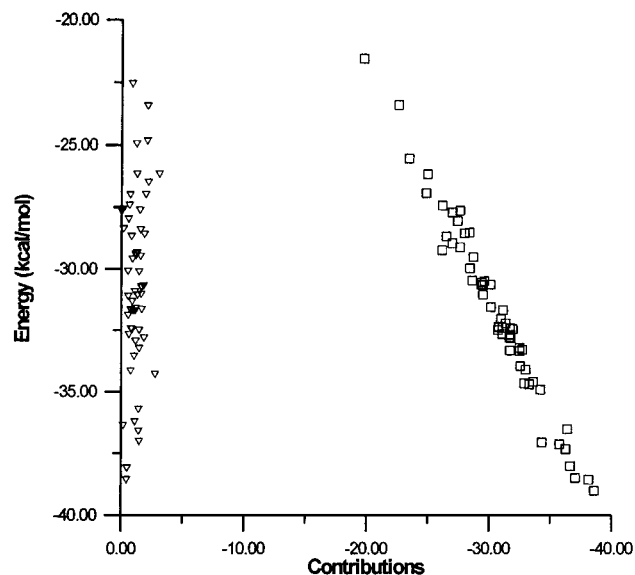
Figure 6. A plot of van der Waals (squares) and electrostatic (triangles) contributions to the interaction energy E (all in kcal mol^{-1}).

Table 7. Comparison of Observed H-Bonds and Those Predicted by Rigid Docking for Roscovitine in Å

	NH(Leu83)···N7 (roscovitine)	O(Leu83)···HN6 (roscovitine)
observed	3.38	2.82
predicted	3.28	3.21

derivatives were more negative than the roscovitine interaction energy. Nevertheless, we have found a few substituents for which the interaction energies are even higher than those calculated for the roscovitine (see Table 6).

The cdk1 and cdk2 assays showed that C2-substitution may increase the inhibitory activity. The docking experiments confirm this observation (Table 4). Therefore, finding an appropriate C2 substituent seems to be a suitable approach to designing new potent and selective inhibitors. The first step in any such a design is to make sure that the space occupied by the roscovitine C2 chain is the same as the space occupied by the ATP N9-substituent and by the IPA 6-substituent (Figure 3).

It is known that addition of a methyl substituent at positions 1, 3, and 7 drastically reduces the cdk1 activity. Our docking experiments are not able to explain this experimental observation, because the interaction energies calculated for the 1-methyl and 3-methyl roscovitine derivatives are −39.0 and −32.6 kcal mol^{-1}, respectively, which is too low (even more negative than for the roscovitine complex). These derivatives keep the same binding mode as roscovitine.

Binding of the Ligand to the Active Site. The interaction energy of 2,6,9-purine derivatives has two considerable contributions, electrostatic and van der Waals, where the electrostatic contribution includes the H-bonds. The rigid docking experiments show that the electrostatic contribution is small and almost substituent-independent (being in the range from −3.1 to −2.0 kcal mol^{-1}). The increase or decrease in interaction energy is caused by the van der Waals contribution, which is about 10-fold higher than the electrostatic contribution (from −38.6 to −19.7 kcal mol^{-1}). Figure 6 shows these two contributions to the interaction energy. The H-bonds predicted by rigid docking are in good agreement with the experimentally observed ones (Table 7).

Binding Modes. The active site of cdk2 offers many different binding modes for purine derivatives that are strongly dependent on the purine substituent. This

observation results from the comparison of ligand orientations in the active site for known ligand−cdk2 complexes (Figure 3). The results of rigid docking show two different binding modes; the first is similar to the crystal orientation of roscovitine and the second to ATP orientation. The mean interaction energy of crystal roscovitine-like orientation is −77.8 kcal mol^{-1} (1.2 Å rmsd) and the interaction energy of ATP crystal-like orientation is −55.4 kcal mol^{-1} (2.8 Å rmsd).

These two binding modes were also found by flexible docking. The first one was very similar to roscovitine crystal orientation and its binding energy was equal to −74.6 kcal mol^{-1} (2.1 Å rmsd). The second one corresponded to the ATP crystal orientation (with binding energy −73.4 kcal mol^{-1} and 2.6 Å rmsd). In the ATP-like binding mode the roscovitine was positioned a little away from the cavity because a large substituent (N^6-benzyl) was present at the N^6-position of adenine. It was observed that the docked conformations did not agree with the conformation of roscovitine in the crystal. There were considerable differences in N9-isopropyl orientation and in C2 side chain shape (Figure 7). The results obtained after the C2-isopropyl fixation showed also two ATP- and roscovitine-like (Figure 8) binding modes. The roscovitine-like interaction energy was equal to −77.2 kcal mol^{-1} (1.5 Å rmsd), but the structure with the lowest interaction energy (−78.2 kcal mol^{-1}) was positioned differently from the roscovitine binding mode.

Conclusions

We have used rigid and flexible docking techniques for prediction of cdk2 and cdk1 inhibitory activities. The parameters for the rigid docking were optimized to allow us routine work. After that, 47 docking experiments were performed with the cdk2 active site. We have calculated the rank correlation between the interaction energy and the respective cdk2/cdk1 assayed activity. The calculated correlation coefficients imply that the rigid docking is a suitable technique for making qualitative predictions about activity. At the same time, the results confirm the assumption that there is a considerable relationship between the cdk1 activity and the cdk2 interaction energy.

We have studied also the influence of the substitution of the purine ring on ligand interaction energy and attempted to predict new possibly active N9-derivatives. The docking experiments did not explain the experimentally observed inactivity of N1 and N3 purine derivatives, because the interaction energies calculated for these compounds are inadequately high.

Information obtained in this study will be used for designing new active anticancer compounds and for additional work in the area of docking experiments. Even now, the combination of medicinal chemistry, X-ray data, and molecular modeling allows us to propose new higly active purine derivatives (e.g. compound **10**) and to prove the usefulness of this approach by synthesizing just a small number of designed compounds.
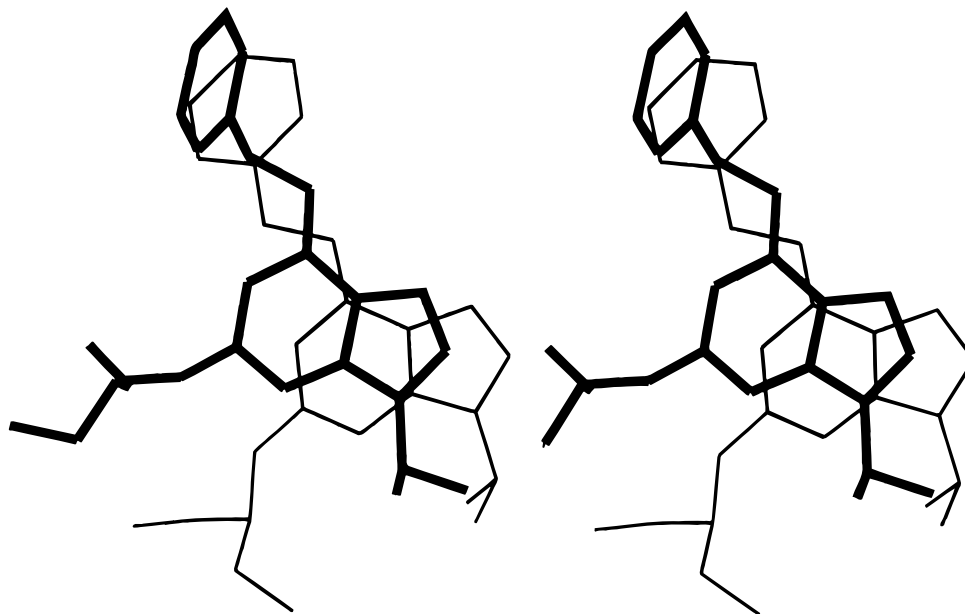
Figure 7. Comparison of the conformation of the lowest energy flexible dock (thick lines) with the crystal conformation (thin lines).
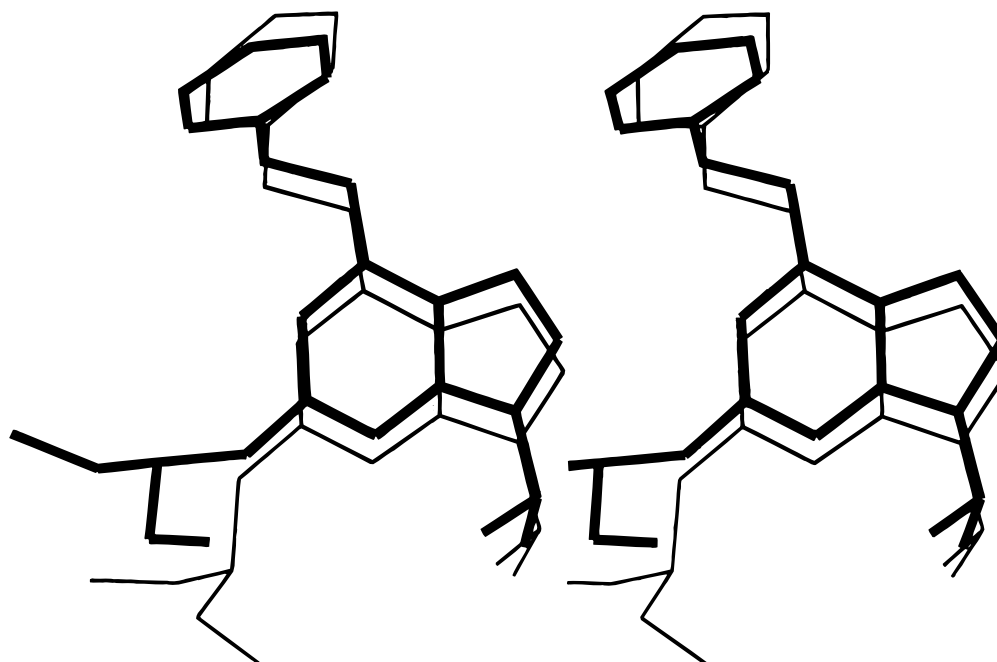
Figure 8. Comparison of the conformation of the second lowest energy dock after N9-isopropyl fixation (thick lines) with the crystal conformation (thin lines).

Experimental Section

cdk2/Cyclin E Kinase Inhibition Assay. Nine compounds were tested for cdk2/cyclin E inhibitory activity to determine the basic relationships between their interaction energies in the docked complex and the inhibitory activity. The cdk2/cyclin E complex was produced in Sf9 insect cells coinfected with an appropriate baculoviral construct. The cells were harvested 70 h postinfection in lysis buffer [50 mM Tris (pH 7.4), 150 mM NaCl, 5 mM EDTA, 20 mM NaF, 1% Tween 20, protease inhibitors] for 30 min on ice, and the soluble fraction was recovered by centrifugation at 14000g for 10 min. The protein extract was stored at −80 °C until use.

The final point test system for kinase activity measurement was used to carry out experiments on the kinetics under linear conditions. The assay mixture contained 1 mg/mL histone (Sigma Type III-S), 15 μM ATP, 0.2 μCi [γ-^{32}P]ATP, and the tested compound in a final volume of 20 μL, all in reaction buffer [50 mM Hepes (pH 7.4), 10 mM MgCl$_2$, 5 mM EGTA, 10 mM 2-glycerolphosphate, 1 mM NaF, 1 mM DTT, and protease inhibitors]. After 10 min, the incubations were stopped by adding SDS sample buffer, and the proteins were separated using 12.5% SDS−PAGE. The measurement of kinase inhibition employed the digital imaging analyzer BAS 1800. The kinase activity was expressed as a percentage of maximum activity and the IC$_{50}$ value was determined by graphic analysis. The cdk1 kinase inhibition tests were done in a similar way.[20]

Synthesis. Melting points were determined on a Kofler block and are uncorrected. The ^{1}H NMR spectra (δ, ppm; J, Hz) were measured on Varian VXR-400 (400 MHz) or on Varian Unity 200 (200 MHz) instruments. All spectra were obtained at 25 °C using tetramethylsilane as an internal

standard. Electron impact mass spectra *m/z* (rel %) were measured on a VG 7070E spectrometer (70 eV, 200 °C, direct inlet). Merck silica gel Kieselgel 60 (230−400 mesh) was used for column chromatography. All compounds gave satisfactory elemental analyses (0.4%).

The following compounds were prepared as described in the literature: 6-(benzylamino)-2-[(3-hydroxypropyl)amino]-9-iso-propylpurine (**1**),[21] 6-(benzylamino)-2(*R*)-[(2-hydroxypropyl)-amino]-9-isopropylpurine (**2**) [mp 142−143 °C, [α] = −8,0 (*c* = 0.11, CHCl₃); prepared in the same way as its racemate synthesized previously[20] by using (R)-(−)-1-amino-2-propanol instead of racemate], 6-(benzylamino)-2-[(2-hydroxyethyl)-amino]-9-isopropylpurine (**4**),[20] and 6-benzylamino-2-[(2-hy-droxyethyl)amino]-9-methylpurine (**5**, olomoucine).[22,23] The straightforward three- or two-step synthesis of other C2, C6, and N9-trisubstituted purines was started from commercially available 2,6-dichloropurine or from 2,6-dichloro-9-isopropyl-purine.[21] The latter was used as a parent compound to avoid alkylation of phenolic OH or C6-NH₂ in the synthesis of compounds **3** or **7** and **10**. The starting compounds were reacted with appropriate alkylamine in 1-butanol in the presence of triethylamine (115−120 °C, 3 h)[20,22] or NH₄OH (85 °C, 9 h, preparation comp.**7**). The N9-H derivatives were then alkylated with isopropylbromide (K₂CO₃, DMF, or DMAA).[20,24] The resulting 9-isopropyl-6-alkylamino-2-chloropurine was further reacted with 3-amino-1-propanol (160 °C, 3 h) or (*R/S*)-2-amino-3-methyl-1-butanol (160 °C, 12 h).[20,22−25] The products were purified by column chromatography.

6-(3-Hydroxybenzylamino)-2-[[1-(hydroxymethyl)-2-(methyl)propyl]amino]-9-isopropylpurine (3): Column chromatography (second principal spot) stepwise 0.5, 1, 1.5% MeOH in CHCl₃ with a trace of concentrated NH₄OH; crystallization CHCl₃−Et₂O; yield 30% (based on 2,6-dichloro-9-isopropylpurine); mp 180−181 °C MS: 384 (11, M⁺•), 366 (35), 354 (22), 353 (72), 341 (23), 323 (100), 298 (12), 175 (11), 134 (14), 122 (12), 107 (67). ¹H NMR (399.90 MHz, CDCl₃ 30 °C): 1.016 (6H, d, *J* = 6.9, (C*H₃*)₂CHC*), 1.025 (6H, d, *J* = 6.9, (C*H₃*)₂CHC*), 1.549 (6H, d, *J* = 6.8, (C*H₃*)₂CHN), 1.557 (6H, d, *J* = 6.8, (C*H₃*)₂CHN), 1.969 (1H, sept, *J* = 6.8, (CH₃)C*H*C*), 1.983 (1H, sept, *J* = 6.8, (CH₃)₂C*H*C*), 3.692 (2H, dd, *J* = 8.0, 10.7, C*H*HOH), 3.869 (2H, dd, *J* = 2.8, 10.7, CH*H*OH), 3.917 (2H, m, C*H*CH₂OH), 4.633 (2H, sept, *J* = 6.8, NC*H*(CH₃)₂), 4.56−4.70 (4H, m, C*H₂*NH), 4.933 (2H, d, *J* = 7.2, N*H*C²), 6.234 (2H, br s, N*H*CH₂), 6.746 (2H, ddd, *J* = 1.1, 2.5, 8.1, ArH), 6.848 (2H, ddd, *J* = 1.0, 1.7, 7.5, ArH), 6.871 (2H, m, ArH), 7.131 (2H, dd, *J* = 7.5, 8.1, ArH), 7.560 (2H, s, HC⁸). The proton 2D-COSY spectrum was used for the assignment of signals. Anal. (C₂₀H₂₈N₆O₂) C, H, N.

6-(Cyclopentylamino)-2-[(3-hydroxypropylamino)am-ino]-9-isopropylpurine (6): Column chromatography (step-wise 0, 1, 2% MeOH in CHCl₃); crystallization from ethyl acetate yield 64%; mp 137−139 °C. MS: 318 (100, M⁺•), 317 (9), 288 (10), 287 (10), 275 (12), 274 (18), 273 (33), 250 (7), 219 (17), 206 (33), 205 (21), 192 (13), 163 (14), 134 (15), 43 (29), 41 (16). ¹H NMR (200 MHz, CDCl₃): 1.53 (6H, d, *J* = 6.8, (C*H₃*)₂-CH), 1.55−1.80 (8H, m, cyclopentyl), 2.09 (2H, m, CH₂C*H₂*-CH₂), 3.65 (4H, m, CH₂N + CH₂O), 4.41 (1H, bm, CH in cyclopentyl), 4.59 (1H, sept, *J* = 6.8, C*H*(CH₃)₂), 4.95 (1H, bt, exch H, OH or NH), 5.21 and 5.60 (each bs 1H, NH or OH), 7.51 s (1H, HC⁸). Anal. (C₁₆H₂₆N₆O) C, H, N.

6-Amino-2-(3-hydroxypropylamino)-9-isopropylpu-rine (7): Crystallization from water; recrystallization from MeOH−Et₂O; yield 70%; mp 143−144 °C. MS: 250 (83, M⁺•), 219 (60), 206 (73), 205 (98), 192 (25), 177 (49), 163 (100), 150 (50), 134 (65), 108 (37). ¹NMR (400 MHz, CDCl₃): COSY[1.546 (6H, d, *J* = 6.8, (C*H₃*)₂CH, 4.63 (1H, sept, *J* = 6.8, (CH₃)C*H*)], COSY[1.73 (2H, m, CH₂C*H₂*CH₂), 3.59−3.67 (4H, m, C*H₂*-CH₂C*H₂*)], COSY[7.97 (1H, bt, *J* = 6.7, NH), 3.59−3.67m], 5.4 (bs, 2H, NH₂), 7.575 (1H, HC⁸). Anal. (C₁₁H₁₈N₆O·1.5H₂O) C, H, N.

6-(Adamantylamino)-2-[(3-hydroxypropyl)amino]-9-isopropylpurine (8): Column chromatography stepwise 0, 1, 2% MeOH in CHCl₃; syruplike product; yield 31% ¹H NMR (400 MHz, D₂O): 1.549 (6H, d, *J* = 6.8, (C*H₃*)₂CH), 1.67−1.76

(6H, m, adamantyl), 1.909 (2H, tt, *J* = 7.1, *J* = 6.6, CH₂C*H₂*-CH₂), 2.10 (3H, bs, adamantyl), 2.19 (6H, bs, adamantyl), 3.582 (2H, t, *J* = 7.1, C*H₂*CH₂CH₂), 3.705 (2H, t, *J* = 6.5, CH₂-CH₂C*H₂*), 4.608 (1H, sept, *J* = 6.8, C*H*(CH₃)₂), 8.083 (1H, s, HC⁸). The proton gCOSY experiment was used for the assign-ment of signals. MS (Waters/Micromass, ZMD-detector, direct inlet, ESI, 20 eV, + ions): [M + H]⁺ = 385.5 (100), 386.5 (22). Anal. (C₂₁H₃₂N₆O·H₂O) C, H, N.

6-Benzylamino-9-isopropylpurine (9). 6-Benzylamino-purine (Fluka) was alkylated by isopropyl bromide analogously to 2-chloropurines mentioned above (in DMSO): Column chromatography 2% MeOH in CHCl₃; crystallization CHCl₃−Et₂O; yield 80%; mp 117−118 °C. MS: 267 (100, M⁺•), 266 (14), 225 (20), 224 (61), 162 (12), 120 (17), 119 (9), 106 (59), 93 (10), 91 (33), 65 (10). ¹H NMR (200 MHz, DMSO): 1.45 (6H, d, *J* = 6.8, (C*H₃*)₂CH), 4.53 (1H, sept, *J* = 6.8, C*H*(CH₃)₂), 4.63 (2H, bs, C*H₂*NH), 8.12 and 8.18 (each s 1H, H-8 and H-2). Anal. (C₁₅H₁₇N₅) C, H, N.

6-(2-Hydroxybenzylamino)-2-[[1-(hydroxymethyl)-2-(methyl)propyl]amino]-9-ispropylpurine (10): Column chro-matography stepwise 0, 0.5, 1.0, 2.0% MeOH in CHCl₃; the syrup-like product crystallized after several days, yield 35%; mp 126−138 °C. MS: 384 (19, M⁺•), 366 (7), 353 (25), 341 (10), 298 (13), 274 (38), 260 (25), 217 (20), 192 (15), 175 (32), 134 (20), 107 (36), 78 (35), 69 (35), 55 (44), 43 (98), 41 (100). ¹H NMR (400 MHz, CDCl₃): 1.060 (3H, d, *J* = 6.8, (C*H₃*)₂CHC*), 1.065 (3H, d, *J* = 6.8, (C*H₃*)₂CHC*), 1.515 (3H, d, *J* = 6.8, (C*H₃*)₂CHN), 1.523 (3H, d, *J* = 6.8, (C*H₃*)₂CHN), 2.040 (1H, sept, *J* = 6.8, (CH₃)C*H*C*), 3.743 (1H, dd, *J* = 7.4, 10.6, C*H*HOH), 3.824 (1H, m, CH₂C*H*), 3.890 (1H, dd, *J* = 2.5, 10.6, CH*H*OH), 4.505 (1H, dd, *J* = 6.6, 15.0, C*H*HNH), 4.570 (1H, sept, *J* = 6.8, NC*H*(CH₃)₂), 4.653 (1H, dd, *J* = 7.0, 15.0, CH*H*NH), 5.028 (1H, d, *J* = 6.9, N*H*CH), 6.474 (1H, bs, N*H*CH₂), 6.845 (1H, dt, *J* = 1.2, 7.4, ArH), 6.918 (1H, dd, *J* = 1.2, 8.3, ArH), 7.174−7.222 (2H, m, ArH), 7.498 (1H, s, HC⁸). The proton 2D-COSY, TOCSY, and HMQC experiments were used for the assignment of signals. Anal. (C₂₀H₂₈N₆O₂) C, H, N.

Hardware and Software. The docking experiments as well as receptor and ligand preparations were performed on SGI Indigo² Extreme (R4400), SGI Onyx 2 (R4000), SGI Power Challenge (12 × R10000), DEC Alpha (2 × 250 MHz), and PC (CPU Intel PIII 450) machines. The Insight II (MSI Biosym) software[15] was used for structure manipulation and visualiza-tion of results. The HyperChem 5.01 (HyperCube) software[17] was used for ligand construction and PM3 semiempirical calculations. The molecular docking was performed using DOCK 4.0.1[16] and AutoDock 2.4[18] software packages.

Supporting Information Available: Contact information regarding DOCK, Auto Dock, Insight II, and Hyperchem. This material is available free of charge via the Internet at http://pubs.acs.org.

References

(1) De Azevedo, W. F.; Leclerc, S.; Meijer, L.; Havlíček, L.; Strnad, M.; Kim, S.-H. Inhibition of Cyclin-dependent Kinases by Purine Analogues. *Eur. J. Biochem.* **1997**, *243*, 518−526 (ref 12, Cordon-Cardo, C. *Am. J. Pathol.* **1995** *147*, 545−560, and ref 13, Karp, J. E.; Broder, *S. Nat. Med.* **1995**, *1*, 309−320).

(2) Pindur, U.; Kim, Y.-S.; Mehrabani, F. Advances in Indolo[2,3-a]carbazole Chemistry: Design and Synthesis of Protein Kinase C and Topoisomerase I Inhibitors. *Curr. Med. Chem.* **1999**, *6*, 29–69.

(3) Losiewicz, M. D.; Carlson, B. A.; Kaur, G.; Sausville, E. A.; Worland, P. Potent Inhibition of Cdc2 Kinase Activity by the Flavonoid L86–8275. *Biochim. Biophys. Res. Commun.* **1994**, *201*, 589–595.

(4) Kitagawa, M.; Okabe, T.; Ogino, H.; Matsumoto, H.; Suzuki-Takahashi, I.; Kokubo, T.; Higashi, H.; Saitoh, S.; Taya, Y.; Yasuda, H.; Ohba, Y.; Nishimura, S.; Tanaka, N.; Okuyama, A. Butyrolactone I. A Selective Inhibitor of Cdk2 and Cdc2 kinase. *Oncogene* **1993**, *8*, 2433–2441.

(5) Veselý, J.; Havlíček, L.; Strnad, M.; Blow, J. J.; Donella-Deana, A.; Pinna, L.; Letham, D. S.; Kato, J.-Y.; Detivaud, L.; Leclerc, S.; Meijer, L. Inhibition of Cyclin-Dependent Kinases by Purine Analogues. *Eur. J. Biochem.* **1994**, *224*, 771–786.

(6) Hoessel, R.; Leclerc, S.; Endicott, J. A.; Noble, M.; Lawrie, A.; Tunnah, P.; Leost, M.; Damiens, E.; Dominique, M.; Marko, D.; Niederberger, E.; Tang, W.; Eisenbrand, G.; Meijer, L. Indirubin, the Active Constituent of a Chinese Antileukaemia Medicine, Inhibits Cyclin-dependent Kinases. *Nature Cell. Biol.* **1999**, *1*, 60–67.

(7) Zaharevitz, D. W.; Gussio, R.; Leost, M.; Sanderowitz, A. M.; Lahusen, T.; Kunick, C.; Meijer, L.; Sausville, E. A. Discovery and Initial Characterization of the Paullones, a Novel Class of Small-Molecule Inhibitors of Cyclin-dependent Kinases. *Cancer Res.* **1999**, *59*, 2566–2569.

(8) Kent, L. L.; Hull-Campbell N. E.; Lau T.; Wu, J. C.; Thompson, S. A.; Nori, M. Characterization of Novel Inhibitors of Cyclin-Dependent Kinases. *Biochem. Biophys. Res. Commun.* **1999**, *260*, 768–774.

(9) Gray, N.; Détivaud, L.; Doerig, Ch.; Meijer, L. ATP-site Directed Inhibitors of Cyclin-dependent Kinases. *Curr. Med. Chem.* **1999**, *6*, 859–875.

(10) Lybrand, T. P. Ligand-Protein Docking and Rational Drug Design. *Curr. Opin. Struct. Biol.* **1995**, *5*, 224–228.

(11) Schulze-Gahmen, U.; Brandsen, J.; Jones, H. D.; Morgan, D. O.; Meijer, L.; Veselý, J.; Kim, S.-H. Multiple Modes of Ligand Recognition: Crystal Structure of Cyclin-Dependent Protein Kinase 2 in Complex With ATP and Two Inhibitors, Olomoucine and Isopenthenyladenine. *Proteins: Struct. Func. Genet.* **1995**, *22*, 378–391.

(12) De Azevedo, W. F.; Leclerc, S.; Maijer L.; Havlíček, L.; Strnad, M.; Kim, S.-H. Inhibition of Cyclin-Dependent Kinases by Purine Analogues: Crystal Structure of Human Cdk2 Complexed With Roscovitine. *Eur. J. Biochem.* **1997**, *243*, 518–526.

(13) Kim, S.-H. Structure-Based Inhibitor Design for Cdk2, a Cell Cycle Controlling Protein Kinase. *Pure Appl. Chem.* **1998**, *70*, 555–565.

(14) Noble, M. E. M.; Endicott, J. A. Chemical Inhibitors of Cyclin-Dependent Kinases: Insights into Design from X-ray Crystallographic Studies. *Pharmacol. Theor.* **1999**, *82*, 269–278.

(15) Insight II program 1995 Biosym/MSI, San Diego, USA.

(16) Ewing, T. J. A.; Kuntz, I. D. Critical Evaluation of Search Algorithm for Automated Molecular Docking and Database Screening *J. Comput. Chem.* **1997**, *18*, 1175–1189.

(17) HyperChem 5.01 program 1997 Hypercube Inc., Ontario, Canada.

(18) Goodsell, D. S.; Olson, A. J. Automated Docking of Substrates to Proteins by Simulated Annealing Proteins. *Struct. Func. Genet.* **1990**, *8*, 195–202.

(19) Siegel, S. *Nonparametric Statistics*; McGraw-Hill: New York, 1956.

(20) Havlíček, L.; Hanuš, J.; Veselý, J.; Leclerc, S.; Meijer, L.; Shaw, G.; Strnad, M. Cytokinin-Derived Cyclin-Dependent Kinase Inhibitors: Synthesis and cdc2 Inhibitory Activity of Olomoucine and Related Compounds. *J. Med. Chem.* **1997**, *40*, 408–412.

(21) Havlíček, L.; Hajdúch, M.; Strnad, M. Cyclin-dependent kinase inhibitor. Patent Applied in Australia, Canada, Japan, Korea and USA, 1998, AU5646598.

(22) Hocart, C. H.; Letham, D. S.; Parker, C. W. Substituted Xanthines and Cytokinin Analogues as Inhibitors of Cytokinin N-Glucosylation. *Phytochemistry* **1991**, *30*, 2477–2486.

(23) Parker, C. W.; Entsch, B.; Letham, D. S. Inhibitors of Two Enzymes which Metabolize Cytokinins. *Phytochemistry* **1986**, *25*, 303–310.

(24) Imbach, P.; Capraro, H. G.; Furet, P.; Mett, H.; Meyer, T.; Zimmermann, J. 2,6,9-Trisubstituted Purines: Optimization Towards Highly Potent and Selective CDK1 Inhibitors. *Bioorg. Med. Chem. Lett.* **1999**, *9*, 91–96.

(25) Raiford, L. Ch.; Clark, E. P. Diacyl Derivatives of ortho-hydroxybenzylamine *J. Am. Chem. Soc.* **1923**, *45*, 1738–1745.